

# **A Sparse, Triangle-shaped Sensor Array for Damage Orientation and Characterization of Composite Structures**

**Wen Qiu<sup>1</sup>, Lei Xu<sup>2</sup>, Yaozhong Liao<sup>2</sup>, Qiao Bao<sup>1</sup>, Qiang Wang<sup>1\*</sup>, Zhongqing Su<sup>2</sup>**

1. College of Automation & College of AI, Nanjing University of Posts and Telecommunications, 9 Wenyuan Road, Nanjing, 210046, PR China.
2. Department of Mechanical Engineering, The Hong Kong Polytechnic University, Kowloon, Hong Kong SAR, PR China.

\*Corresponding author: Qiang Wang, E-mail: wangqiang@njupt.edu.cn

## **Abstract**

Since numerous sensors are needed to create a sensor array for the structural health monitoring of large-scale structures, the equipment quantity and cost considerably increase. This study proposes a sparse, triangle-shaped sensor array to identify, orient, and assess the degree of structural damage in composite constructions in order to overcome this shortcoming. The damage-scattered Lamb waves are recorded by the sparse sensor array with a variety of features that are then extracted and fed into the Support Vector Machine (SVM) classification method. The location and severity of the damage in composite constructions can be determined by training the SVM model. The Principle Component Analysis (PCA) technique is used to compress the wave feature vectors while maintaining the majority of the damage information because the high dimension of the wave feature vectors required a significant amount of calculation during the training phase. Proof-of-concept tests show that the trained model, by utilizing the many properties of Lamb wave signals, can orient and define the degree of damage with excellent accuracy. Multiple Lamb wave properties can be used to make up for the triangle sensor array's loss of damage information. In conjunction with the SVM, the triangle-shaped sensor array that was proposed in this study can efficiently make it easier to identify and characterize damage to large-scale structures while using fewer sensors.

**Keywords:** Triangle-shaped sparse sensor array, Composite structures, Lamb waves, Damage identification model

## **1 Introduction**

Composite structures are the fundamental components used in aerospace vehicles, wind turbine blades, ships and other infrastructures. However, such composite structures are vulnerable during manufacturing process and in-service operation, resulting in a sharp decline in structural strength and posing a serious threat to the safety of engineering structures [1]. To avoid catastrophic disasters, intensive effort over the years have been aroused to develop an online damage monitoring system which can be employed to assess the health status of composite structures accurately and timely. Representative approaches include acoustic emission, thermography, vision-based inspection, guided ultrasonic wave (GUW) and so on. Among them, GUW has the outstanding advantages of large detection range, high sensitivity to various types of damage and cost-effectiveness in implementation.

Good supply of study has been conducted that making use of GUWs for damage identification, localization and health monitoring of composite structures. From the perspective of incentive mode, Ghosh and Kundu proposed a new transducer holder mechanism, which provides water coupling between the ultrasonic transducers and the specimen [2]. Compared with conventional ways in detecting objects, this method does not require a water jet or a big tank for immersing the specimen into it, which can be used for monitoring structures with Lamb wave. Jagannathan developed a new compact sensor configuration comprising a single transmitter and multi-receivers (STMIR) for the in-situ structural health monitoring (SHM) of large plate-like isotropic structures [3]. Considering the sensor layout, Kundu et al used two clusters (three sensors in each cluster) to locate the sound source in the large board [4]. Based on this method, Yin proposed a new sensor group orientation, which uses two clusters (four sensors in each cluster) to locate the sound source with higher accuracy [5]. Danilo reported that compared with Lead zirconate titanate (PZT) ceramics, the piezoelectric diaphragms have higher sensitivity in classification of damage in large structures with lower cost, which are suitable to be densely installed to form a sensor network for impedance-based SHM in large structures [6]. Salamone proposed a method

based on an array of macro-fiber composite (MFC) transducers arranged as rosettes for high-speed collision location on isotropic and composite aircraft panels. The experiments reported herein show the applicability of the technique to high-velocity impacts created with a gas-gun firing spherical ice projectiles[7]. An approach based upon the employment of piezoelectric transducer rosettes is proposed for passive damage or impact location in anisotropic or geometrically complex structures. This method is applicable to anisotropic complex structures, and it is challenging for traditional time-of-flight source location due to direction dependent wave velocity[8]. These approaches have shown their capabilities in evaluating the health status of structures. Nevertheless, when the scale of the monitored structure becomes larger or there are multiple areas to be monitored, such composite materials as fan blades and large aircraft wings. The number of sensors, the signal dimensions as well as the calculation amount during the implementation of the current methods would significantly increase, which restrict the application of these methods in practical engineering.

To address the restrictions induced by the above factors and carry out timely identification, evaluation as well as localization of structural damage in composite components, some research has been performed from the perspectives of sensor placement optimization, algorithm development, and data processing. Up to now, a lot of work has been done by using the Lamb wave for damage evaluation and monitoring. Aimed at detecting unknown damage in three-dimensional (3D) heterogeneous structures, a localization is proposed by Kundu and Yin [9]. This technique helps to localize the acoustic source with only a few sensors, which is heuristic for the scenario that limited sensors can be used for the monitoring of structures. Xue *et. al.* focused on the analysis of the positioning error of multi-sensor cluster methods with sensor arrangements of isosceles right-angled triangle and triangular pyramid and used the correction algorithm to improve the locating results [10]. The above studies provide extremely valuable value for large-scale damage research, But, for large structures and multiple monitoring areas, it is still difficult to identify, orientate, and characterize structural damage accurately and timely.

Due to the coupling of multi features of the Lamb waves, the output signals acquired by the sparse sensor array are complex, which are the mixture of linear and nonlinear ultrasound waves. The classification algorithm in machine learning has good applicability to this kind of classification problem. Therefore, a support vector machine (SVM) based algorithm is employed to handle such a complex model. According to the micro characteristics of Reinforced Concrete (RC) frame structure, Su [11] established a sample database and introduced Machine Learning Algorithm, which can accurately predict the vulnerability of the structure. Azadeh Noori Hoshyar [12] compared several nondestructive testing (NDT) methods to detect and visualize damage, and proposed a machine learning method based on SVM to prevent misjudgment of events. Thirumalaiselvi [13] used acoustic emission (AE) technology to evaluate the progressive development and location of damage in concrete structures, and used SVM to classify acoustic emission sources. In his method, a one-to-one combination scheme is adopted, which means a SVM is constructed between any two types of samples. For problems of multiple types, it is necessary to construct multiple SVMs (it is a typical classification algorithm with solid theory and enduring in many classification algorithms), and each trained classifier is used to distinguish one of the two classes.

According to the analysis above, for the large-scale structural damage diagnosis, sparse array seems necessary to well reduce the number of sensors and the signal processing. In this situation, more characteristic parameters should be extracted to indicate the damage factors. By using these new more parameters, damage diagnosis and evaluation can be realized through the classification algorithm of machine learning. To this end, in this paper, a new Lamb wave-based damage detection and evaluation scheme is proposed, in which a triangle-shaped sparse array is employed to acquire the Lamb wave signals. Diverse characteristics of Lamb waves are extracted to compensate the lack of information provided by traditional detection method (such as RMSD), since Lamb waves can maintain a long-distance transmission in large-scale structures. Subsequently, a SVM based damage identification model

is designed to realize the diagnosis of structural damage of composite structures.

## 2 Basic Principle Of Lamb Waves And Damage Monitoring Method

Lamb wave is an elastic wave formed by the coupling of transverse wave and longitudinal wave in a structure with two parallel surfaces. Due to its long propagation distance with low attenuation and sensitivity to small damage, Lamb wave-based damage detection and evaluation has been widely used in prevailing SHM frameworks [14-18]. Conventional sensor networks utilized in Lamb wave-based SHM systems are normally complicated and onerous, which requires a large number of PZT sensors, as illustrated in Fig. 1. Each PZT sensor work as both the wave actuator and receiver. Lamb waves, which are emitted into the monitored structure via a PZT wafer, can induce physical disturbances to interrogate the structure. Upon interacting with structural damage, Lamb waves are modulated and the damage information will be embodied in the distorted wave signals. By extracting and analysing damage-distorted signals, structural damage can be identified, characterized, and localized in conjunction with appropriate algorithms.

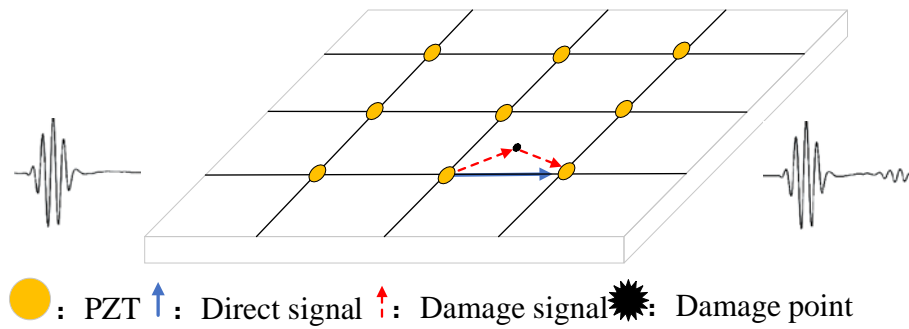


Figure 1. Principle of Lamb waves based damage monitoring

With an increase in the size of the structure or the areas to be monitored, it is possible to notice an

exponential development in the number of sensors, which results in increased weight, volume, and cost penalties. In the meantime, such a vast sensor network will export a lot of duplicated data, which could make data processing more difficult [19-21]. Therefore, one of the most crucial goals for expanding the use of Lamb wave-based SHM systems in constructing composite structures is to develop an efficient sparse sensor network.

Considering that the small-scale structural damage has ignorable effect on the health of large-scale structure, more attention should be paid to the regional major damage as well as its progressive growth and evolution. In this scenario, sparse sensor network is a more suitable candidate, compared with a dense sensor network. An important issue that a sparse sensor network will cause is that the damage information extracted from the captured wave signals is insufficient due to the reduction of the number of sensors, and the accuracy of the damage detection and characterization can be affected owing to the insufficiency of the damage information. Therefore, to compensate for the deficiency of the damage information, more clues about the structural damage need to be dug out based on the limited wave signals captured by the sparse sensor network.

A crucial task in SHM is the quantitative assessment of damage degree, in addition to the identifying and locating them. Machine learning classification techniques are very suitable for such problems. In this study, the damage degree was quantitatively evaluated by using four classification algorithms: decision tree, linear discriminant, SVM, and KNN. Based on the experimental results, it is discovered that SVM performs better than the other three algorithms, demonstrating that the proposed triangle-shaped sensor array in conjunction with SVM can efficiently locate, characterize, and identify structural damage in large-scale composite structures.

### **3 Composite structural health monitoring based on sparse array**

In view of the above analysis, the damage information carried by Lamb wave is quite rich. Therefore, mining more hidden characteristic parameters and establishing the damage characteristic parameter set

can comprehensively distinguish the damage. In the face of such large-scale structure, through reasonable sensor layout, the most simplified sparse array is adopted here, that is, three sensors, which can not only reduce the number of sensors, but also complement each other with rich characteristic parameters. Complete the establishment of damage location evaluation model and finally complete the method design. The specific design idea is shown in Figure 2.

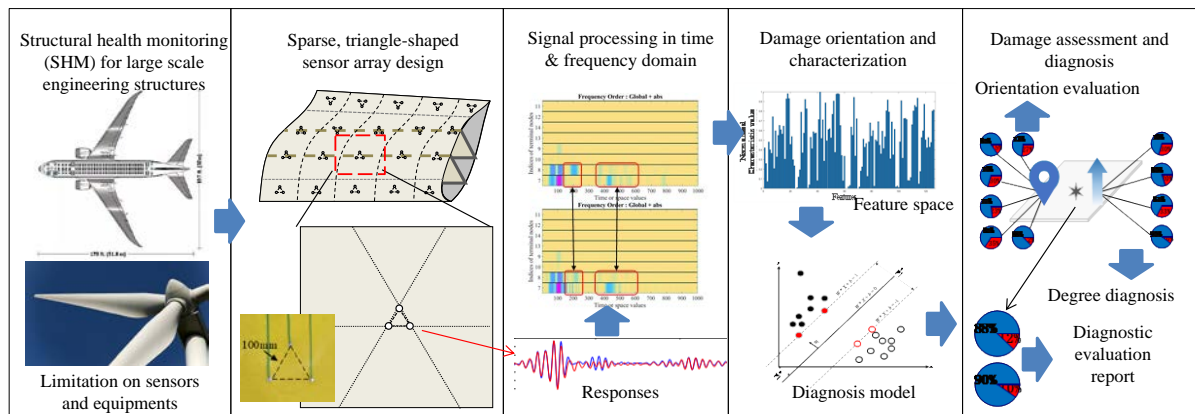
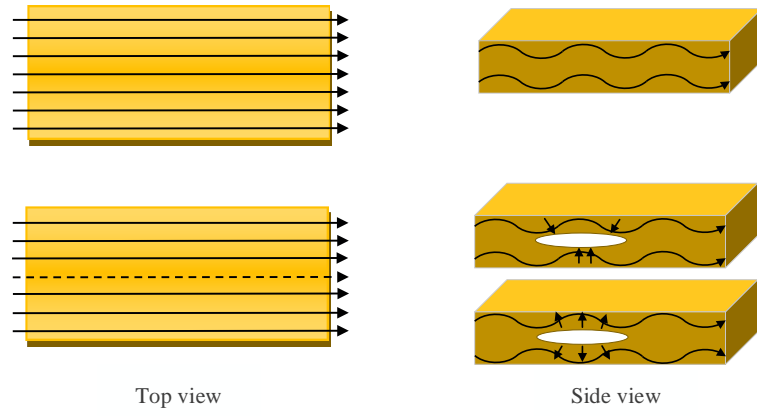


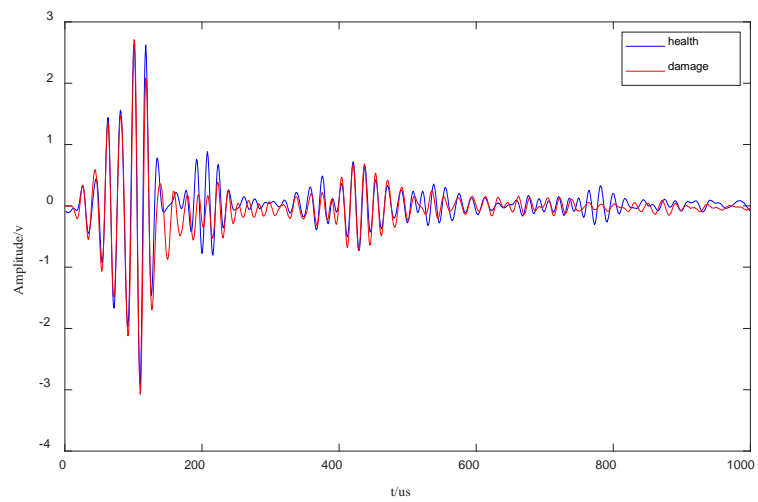
Figure 2. Overall design idea

### 3.1 Influence of damage on Lamb wave propagation

Taking the delamination as a representative structural damage, the Lamb wave is interfered by the delamination, resulting in a changed propagation path and a modulated waveform, as shown in Fig. 3(a) and Fig. 3(b), respectively. Typical Lamb wave signals captured in an intact and a damaged composite structure are displayed in Fig. 3(b). It can be observed that obvious deviations between the two signals are caused due to the existence of delamination, indicating that useful damage-related information can be extracted for damage identification and localization.

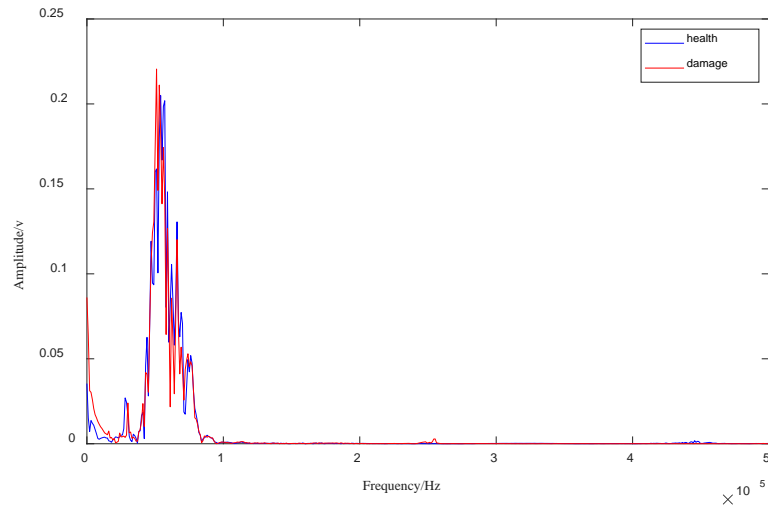


(a) Schematic diagram of wave propagation in an intact and a damaged composite structure

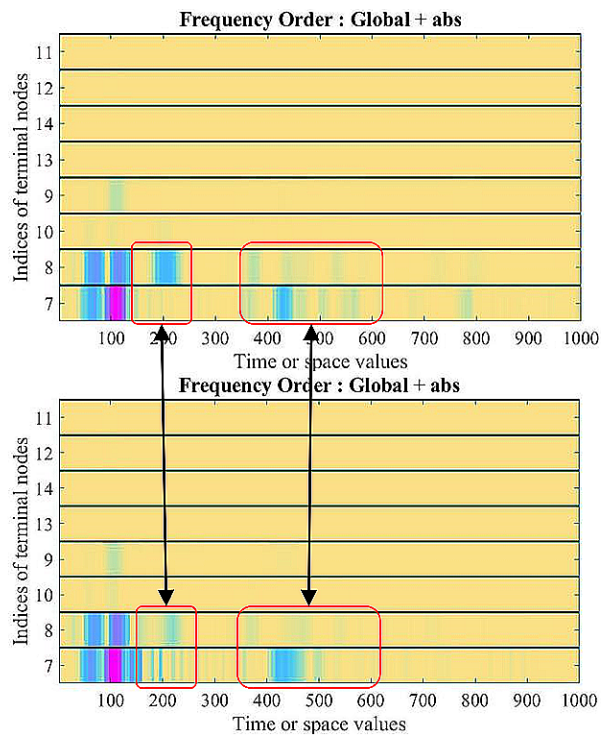


(b) Typical time domain waveform in an intact and a damaged composite structure

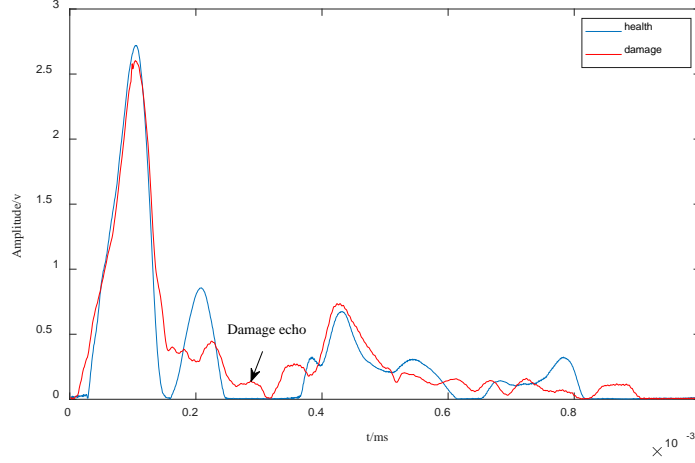




(c) Time domain spectra of the wave signals captured from intact and damaged structures respectively



(d) Time-frequency domain spectra of the wave signals captured from intact and damaged structures, respectively



(e) Comparison of IMF1 transient amplitudes between healthy and damage signals

Figure 3. Difference between health and damage structures

### 3.2 Multi feature parameters extraction

The magnitudes of the collected wave signals will diminish because of the energy dissipation caused by the damage since the majority of the Lamb wave will traverse the damage while a portion of the wave will be reflected by the damage. By taking Discrete Fourier Transform(DFT), the spectra of the captured wave signals in frequency domain can be obtained, as shown in Fig. 3(c). It can be observed that variations of the spectra of the wave signals captured from intact and damaged structures are caused around the fundamental frequency, due to the interaction of probing Lamb waves and the damage. Via wavelet packet transform, the spectra of the captured wave signals in the time-frequency domain can be obtained, as displayed in Fig. 3(d). By decomposing the wave signals into different frequency bands, a variety of time-frequency features (e.g., wavelet energy ratio, wavelet energy entropy) of the wave signals can be extracted, which can be utilized as the input of a SVM for damage identification and localization. In addition, the energy envelopes of the captured wave signals can be ascertained by utilizing Hilbert transform, as shown in Fig. 3(e). It can be observed that due to the damage-induced wave scattering, the instantaneous amplitude of Intrinsic Mode Function 1 (IMF1) of the wave signal captured from damaged

structure is significantly larger than that of the wave signal captured from the intact structure, which can also be used in SVMs for damage evaluation.

The position and the severity of the damage can be determined and characterized by extracting the damage-induced information from these captured wave signals. In this work, four categories with totally 42 features are extracted from the captured wave signals, as shown in Table 1, which are utilized as the input parameters of SVMs to identify and localize the damage in the monitored structure. Due to the large number of extracted features and redundant behavior, better feature deletion and selection will be carried out in the later stage.

Table 1. Multi parameter features

| <b>Time Domain Features</b>          | <i>max amplitude</i>           | <b>Frequency Domain Features</b>            |
|--------------------------------------|--------------------------------|---|
| <i>signal envelope area</i>          | <i>impulse factor</i>          | <i>gravity frequency</i>                    |
| <i>signal correlation</i>            | <i>clearance factor</i>        | <i>frequency variance</i>                   |
| <i>signal difference coefficient</i> | <i>waveform factor</i>         | <i>mean square frequency</i>                |
| <i>root mean square</i>              | <i>fractal dimension</i>       | <b>Time-Frequency Features</b>              |
| <i>frequency variance</i>            | <b>Multi Signal Features</b>   | <i>wavelet energy ratio</i>                 |
| <i>skewness</i>                      | <i>arrival time eigenvalue</i> | <i>wavelet energy entropy</i>               |
| <i>peak factor</i>                   | <i>signal mutation time</i>    | <i>wavelet characteristic scale entropy</i> |
| <i>kurtosis</i>                      | <i>signal difference</i>       | <i>wavelet singular spectral entropy</i>    |
| <i>peak to peak</i>                  | <i>scattering signal size</i>  | <i>imfl mean</i>                            |
| <i>factor K</i>                      | <i>scattering wave packet</i>  |   |

### 1) Wavelet energy ratio

Supposing the data length of the original signal  $S(t)$  is  $N$ , the data length of the discrete signal  $S_{(j,k)}(i)$  in the decomposed frequency band is reduced to  $2^{-j}N$ . Thus, its energy can be expressed as:

$$E(S_{(j,k)}(i)) = \frac{1}{2^{-j}N-1} \sum_{i=1}^{2^{-j}N} (S_{(j,k)}(i))^2 \quad (1)$$

where,  $j$  is the number of decomposition and  $k= 0,1,2, \dots, 2j-1$  is the position index of decomposition frequency band.

The energy proportion of the  $k$  band decomposed signal is as follows:

$$E_m = \frac{E(S_{(j,k)}(i))}{E(S(t))} \quad (2)$$

where,  $E(S(t))$  is the sum of total energy.

## 2) Wavelet energy entropy

After obtaining the energy proportion of each frequency band of wavelet packet decomposition, the formula of wavelet energy entropy is illustrated as:

$$W_{EE} = - \sum_{i=1}^N E_m \log E_m \quad (3)$$

where,  $E_m$  is the wavelet energy ratio.

## 3) Wavelet characteristic scale entropy

The signal is decomposed by layer  $j$  wavelet packet, and the decomposed subsequence is  $S_{(j,k)}$ , where  $k=0,1,2,\dots,2^j-1$ . The wavelet packet decomposition of the signal is regarded as a division of time domain angle, and the division method is described as:

$$\varepsilon_{(j,k)} = \frac{S_{F(j,k)}(i)}{\sum_{i=1}^N S_{F(j,k)}(i)} \quad (4)$$

where,  $S_{F(j,k)}(i)$  is the  $i$ -th value of Fourier transform sequence of subsequence  $S_{(j,k)}$ . According to the basic theory of information entropy, the characteristic entropy of wavelet packet is defined as:

$$H_{j,k} = - \sum_{i=1}^N \varepsilon_{(j,k)}(i) \log \varepsilon_{(j,k)}(i) \quad (5)$$

where:  $H_{j,k}$  is the entropy value of the characteristic scale of the  $k$ -th wavelet packet in the  $j$ -th layer of the damage signal of the composite plate.

#### 4) Wavelet singular spectral entropy

A window function with a length of  $M$  and a step of size 1 is employed to formulate the subsequence  $S_{(j,k)}$ , and mapped into the embedding space. Then, the coefficient sequence is divided into  $2^jN-M+1$  data segments, and the state matrix is constructed as:

$$A_{j,k} = \begin{bmatrix} S_{(j,k)}^{(1)} & S_{(j,k)}^{(2)} & \cdots & S_{(j,k)}^{(M)} \\ S_{(j,k)}^{(2)} & S_{(j,k)}^{(3)} & \cdots & S_{(j,k)}^{(M+1)} \\ \vdots & \vdots & \ddots & \vdots \\ S_{(j,k)}^{(2^jN-M+1)} & S_{(j,k)}^{(2^jN-M+2)} & \cdots & S_{(j,k)}^{(2^jN)} \end{bmatrix} \quad (6)$$

After decomposing the singular value of  $A_{j,k}$ , the singular value is  $\lambda_{j,k}^m (1 \leq m \leq \min(M, 2^jN-M+1))$ , in which  $\lambda_{j,k}^m$  is the singular value spectrum of the layer signal. The number of non-zero singular values reflects the number of different patterns contained in matrix  $A_{j,k}$ , and the size of singular value  $\lambda_{j,k}^m$  reflects the proportion of corresponding patterns in the total pattern. Therefore, based on the information entropy theory, the singular value spectral entropy of the scale coefficient sequence can be expressed via the following equation as:

$$H_{j,k}(f) = - \sum_{m=1}^{m_0} p_{(j,k)}^m \ln p_{(j,k)}^m \quad (7)$$

where:  $p_{(j,k)}^m = \lambda_{j,k}^m / \sum_{m=1}^{m_0} \lambda_{j,k}^m$ . On the basis of synthesizing redundant information, the singular entropy of wavelet packet space directly reflects the uncertainty of energy distribution of characteristic modes in the time-frequency space of the analyzed signal.

In conclusion, adequate information about the structural damage can be acquired by extracting the multiple features of the wave signals captured by the sparse, triangle-shaped sensor array, to compensate the information loss caused by the reduction of sensor number.

### 3.3 Layout of the triangle-shape sensor array

Considering the large number of sensors of the conventional sensor arrays for large-scale structures and the resultant high extra weight, in this study, a sparse, triangle-shaped sensor array consisting of only three sensors, is designed for the damage identification and characterization of composite structures. The three sensors of the sparse sensor array form an equilateral triangle. According to the sum and delay algorithm [22-24], three damage probability ellipses can be depicted based on the three sensors and the damage position can be pinpointed based on these ellipses. Compared with conventional sensor networks for large-scale structures, a much simpler sensing network can be arranged in each monitoring region by using the proposed triangle-shaped sensor array, as shown in Fig. 4. The number of sensors decreased by about 92%. Via extracting multiple features of the wave signals captured by the sensor array mentioned in section 3.2, the information loss due to the reduction of sensors can be compensated, thus, the structural damage can be identified and characterized with high accuracy.

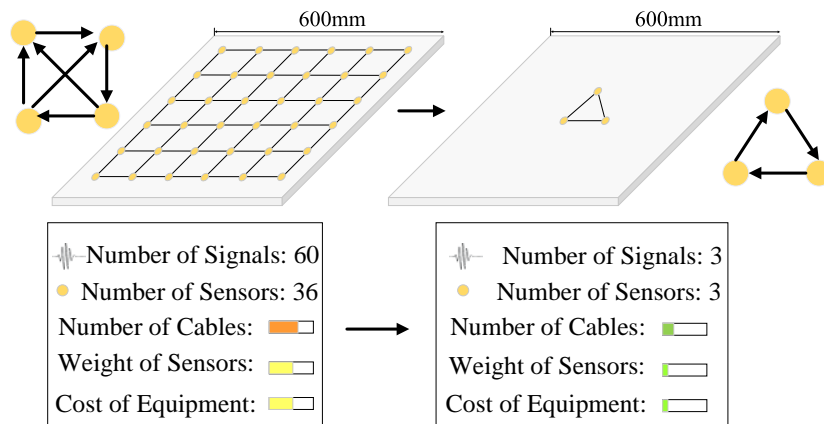


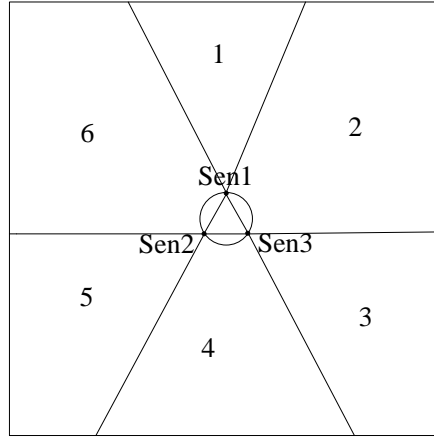
Figure 4. Triangle-shaped sensor array network and regional unit layout

### 3.4 Damage orientation and characterization using classification algorithms

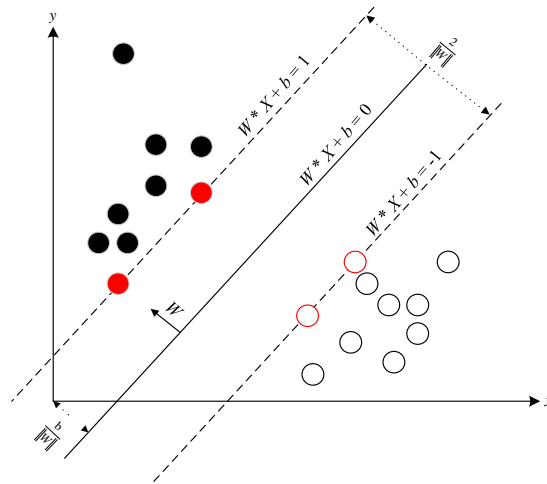
#### 1) Damage position identification

In order to monitor the health state of the structure, the whole structure can be divided into six monitoring regions based on the layout of the triangle-shaped sparse sensor array, as shown in Fig. 5(a). In this method, the damage's location can be identified by comparing the variations in Lamb waves

scattered by the damage in various areas.



(a). Six damage regions divided based on the layout of the triangle-shaped sparse sensor array



(b). SVM schematic diagram

Figure 5 Damage orientation and characterization by using triangle-shaped sparse sensor array and SVM

SVM is widely used in statistical classification and regression analysis, via which a higher-dimensional space and a hyperplane can be established with maximum spacing in this space, as shown in Fig. 5(b). However, it is a multi-stage classification problem to determine the damage location. To deal

with this issue, it is necessary to use several SVMs to form a multi-stage classifier. In this paper, the SVMs are constructed based on one-to-one (one-to-other) principle.

In this study, a total number of  $N$  training samples are studied, in which the samples are symbolized as  $(x_1, y_1), (x_2, y_2), (x_3, y_3), \dots, (x_n, y_n)$ . Taking the  $j$ -th and the  $k$ -th samples as examples, the SVM demand solution between them can be derived as[13]:

$$\begin{cases} w^{jk}, b^{jk}, \xi^{jk} \left\{ \frac{1}{2} \|w^{jk}\|^2 + c \sum_{i=1}^N \xi_i^{jk} \right\} \\ s.t. (w^{jk} \cdot \Phi(x_i)) + b^{jk} \geq 1 - \xi_i^{jk} & y_i = j \\ (w^{jk} \cdot \Phi(x_i)) + b^{jk} \leq 1 + \xi_i^{jk} & y_i = k \\ \xi_i^{jk} \geq 0 & j = 1, \dots, L \quad k = j + 1, \dots, L \end{cases} \quad (8)$$

where,  $w^{jk}$  is the weight vector of the SVM distinguishing the  $j$ -th and  $k$ -th samples;  $b^{jk}$  is the bias value of the SVM;  $\xi_i^{jk}$  is the SVM slack variable;  $\Phi(x_i)$  represents the mapping of  $x_i$  to High-dimensional space. The final decision function is as follows:

$$f_{jk}(x) = \text{sgn}(w^{jk} \cdot \Phi(x_i)) + b^{jk} \quad (9)$$

During the monitoring of damage in composite structures all  $L(L-1)/2$  classifiers are adopted to impel the voting method to make decisions for an unknown damage sample, which means, each classifier judges its own category and votes for the corresponding category. Finally, the unknown sample can be classified into the region with the highest votes.

## 2) Assessment of damage degree

SVM can be used to track and evaluate the evolution of the damage process after determining the position of the damage. As previously stated in section 3.2, only a subset of the 42 characteristics is used and analyzed to determine the damage position. Because the damage status will be changed caused by the ambient environment, the degree of the damage will be accumulated during the working period. Thus, it's difficult to judge the damage timely. Therefore, tremendous information is needed for the evaluation of damage, especially for the structures in a complex environment. For the setting of damage degree, the



identification is based on the determined position. So, as long as the simulation training focuses on four stages with different damage degrees at the same position, sample analysis can be carried out.

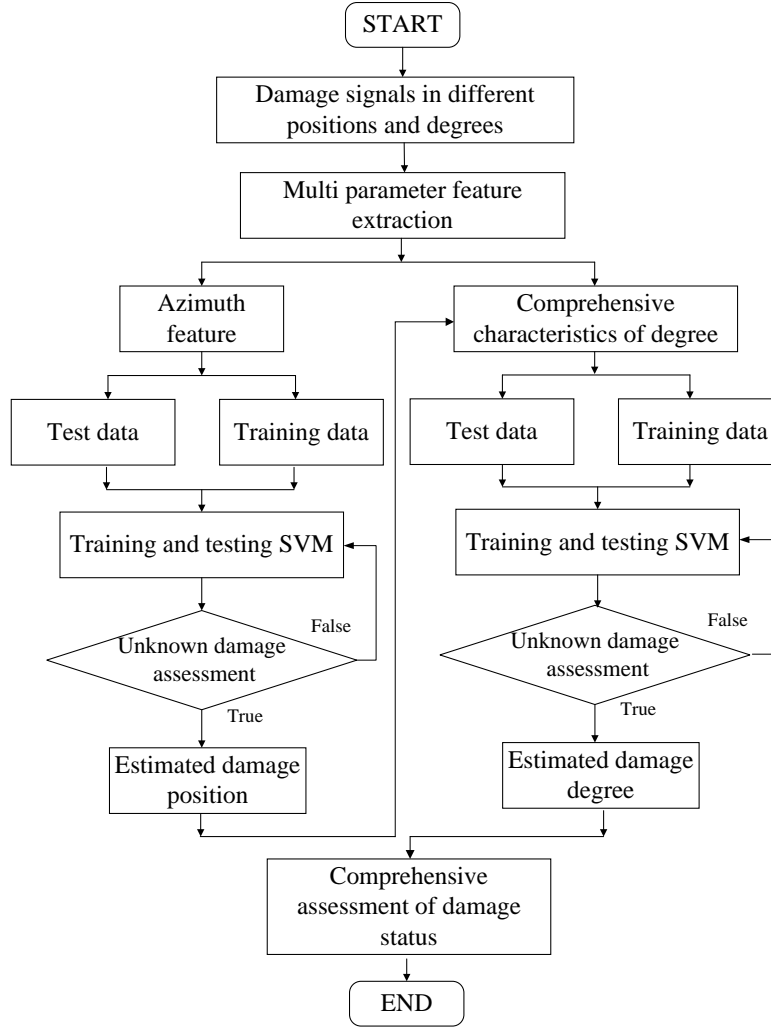


Figure 6. Damage assessment flow chart

According to the specific situation of the occurrence and development of the damage, the lifespan of a structure can be roughly divided into four stages, including the health stage without damage, the embryonic state of damage, the formative stage of damage, and the final stage of damage. The sample space can be written as  $(x_{11}, \dots, x_{1n}, y_i)$ ,  $(x_{21}, \dots, x_{2n}, y_i)$ ,  $\dots$ ,  $(x_{n1}, \dots, x_{nn}, y_i)$ , which are the total parameter space of the time domain, frequency domain, time-frequency domain eigenvalues and multiple signals

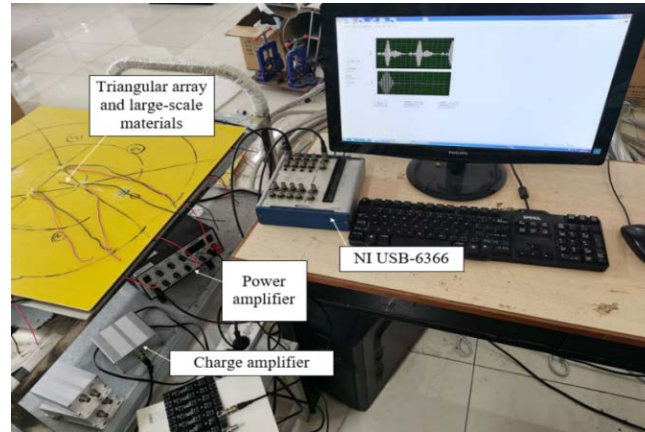
extracted above, in which  $y_i \in \{0,1,2,3\}$  is referred to the label of the four stages. With the help of the multi-input and multi-output model developed from SVM introduced above, 126 characteristic parameter input and 4 result output models are established. The specific process of damage experiment is shown in the Fig. 6.

## **4 Proof-of-Concept Experimental Validation**

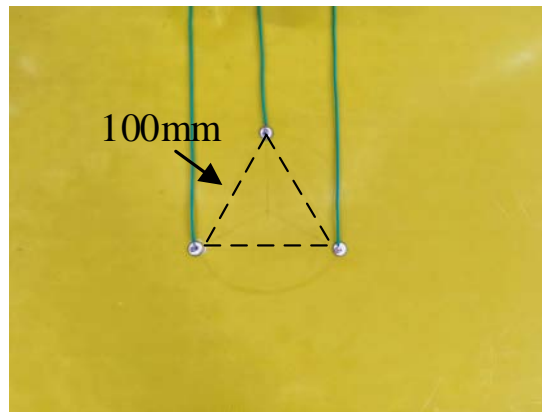
### **4.1 Experimental system and process**

The damage assessment system proposed in this paper includes three modules: i) signal acquisition module, ii) signal processing module, and iii) damage assessment module[25-30]. The signal acquisition module is composed of data acquisition equipment, power amplifier, charge amplifier. The power amplifier is used to amplify the excitation signals. The charge amplifier is used to amplify and filter. In the signal processing module, the acquired signals are analyzed and the characteristic features of wave signals are extracted to establish a damage information database, to further identify and localize the damage. A SVM is employed in the damage assessment module to characterize the degree of damage. The damage sample set is selected from the damage information database, which is further divided into training set and test set to train and test the SVM. Finally, the unknown damage is identified and localized using the proposed damage assessment system, to verify the effectiveness and accuracy of the system.

The specimen used in the experiment is an epoxy resin-glass plate (density: 1960kg/m<sup>3</sup>; Young's modulus: 20 GPa; Poisson's ratio: 0.17) with a size of 600 mm × 600 mm × 3 mm. The excitation signal – a 5-cycle Hanning-windowed sinusoidal toneburst, is generated by the Labview, with a central frequency of 60 kHz. Fig. 7(a) shows the experimental set-up. A triangle-shaped sparse sensor array is arranged in the center of the structure, and the distances between the three sensors are all 100mm, as shown in Fig. 7(b).



(a). Experimental set-up



(b). Layout of the triangle-shaped sparse sensor array

Figure 7 Experimental system

## 4.2 Analysis of experimental results

### 1) Identification of the damage orientation

According to the symmetry of equilateral triangle, the above-mentioned 6 regions are mutually symmetrical with the same properties, namely regions 2 and 5, regions 1 and 4, and regions 3 and 6. Thus, three typical positions are selected for analysis. Firstly, two nonidentical damage in regions 2 and 4 which are investigated, are shown in Fig. 8.

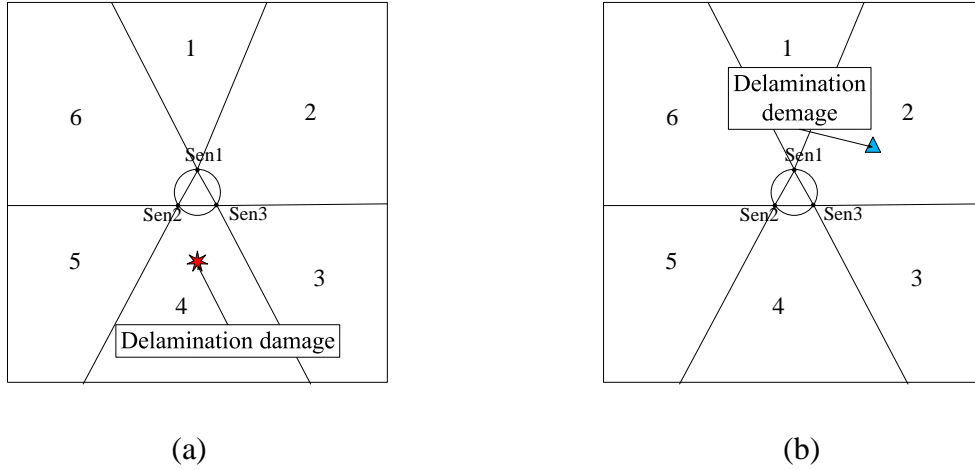
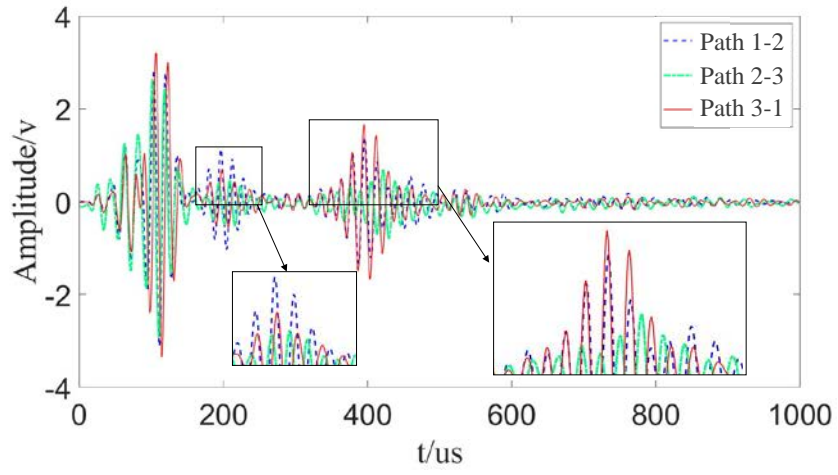
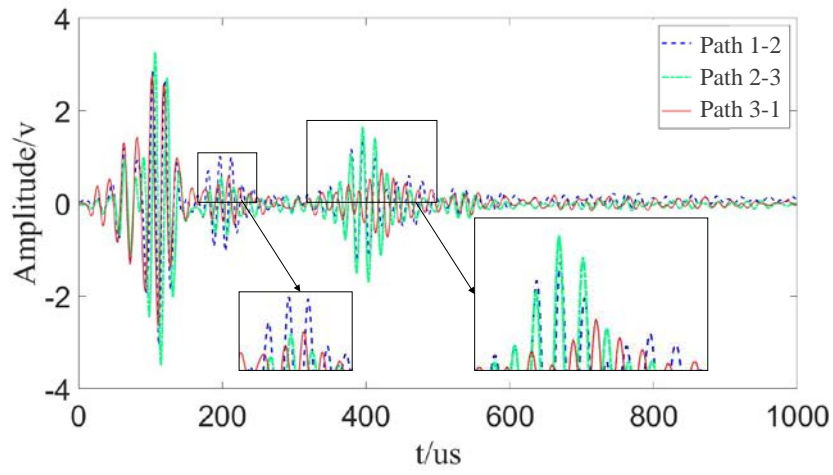


Figure 8. Schematic of the two damage in (a) region 2 and (b) region 4

Fig. 9 depicts the time domain Lamb wave signals acquired by the triangle-shaped sparse sensor array. It can be observed from Fig. 9(a) that if there exists a damage in region 4, the amplitude of the wave signal acquired from path 2-3 (namely, Sen2 is the actuator and Sen3 is the receiver) decrease dramatically compared with that acquired from path 1-2 and path 3-1. As the damage is closest to path 2-3, the effect of damage-induced wave scattering on path 2-3 is stronger than path 1-2 and path 3-1, resulting in a lower wave amplitude in path 2-3. the wave signal acquired from path 3-1 is the lowest among the signals acquired from the 3 paths, as illustrated in Fig. 9(b), which further confirms the above interpretation. The histogram of wave signal difference eigenvalues is shown in Fig. 10.



(a)



(b)

Figure 9. Wave signals captured by the three paths of the sensor array when the damage is in (a) region 4 and (b) region 2

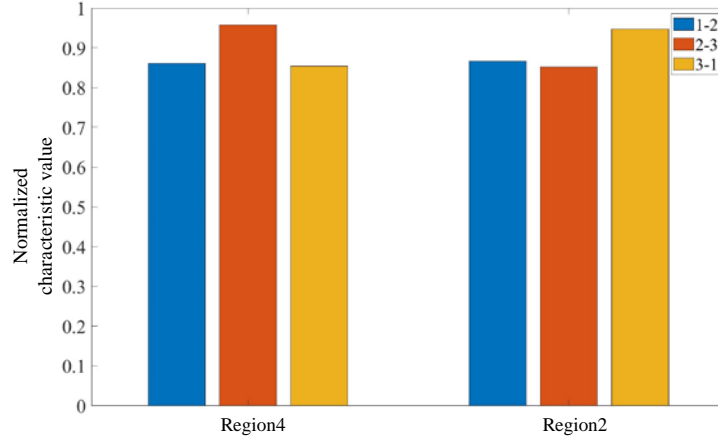


Figure 10. Histogram of wave signal difference eigenvalues

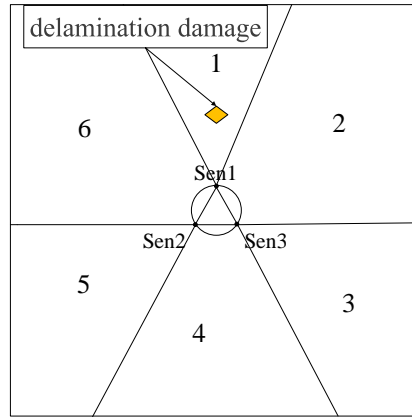


Figure 11. Schematic diagram of damage distribution in zone 1

Further, considering the fact that regions 1 and 4 are symmetric about path 2-3 and the damage in these two regions has a similar impact on wave propagation in path 2-3, it is challenging to identify which region the damage is located in by examining the wave signals obtained from path 2-3. However, the distances between the two damage points and sensors are different, Therefore, it can be further confirmed by the signals acquired by path 1-2 and path 3-1. Fig.12 displays the damage-scattered waves (the red rectangle) and the boundary-reflected waves (the blue dashed rectangle) when the damage is located in region 1. In the red rectangle, the arrival time of the damage-scattered wave captured by path 1-2 is faster

than that of the other two paths due to the damage is closest to path 1-2. In the blue dashed rectangle, the amplitude of boundary-reflected wave captured by path 1-2 is the smallest among the three paths, due to the wave is scattered by the damage before striking the boundary. The normalized characteristic values of the scattering wave packet (SWP) and the arrival time eigenvalues (ATEs) of paths 1-2 and 3-1 are shown in Fig. 13, The figure well reflects the difference of damage characteristics under symmetrical state. When damage is occurred in region 4, the characteristic parameters of paths 1-2 and 3-1 are relatively smaller. On another side, when damage is occurred in region 1, the characteristic parameters of paths 1-2 and 3-1 are relatively larger.

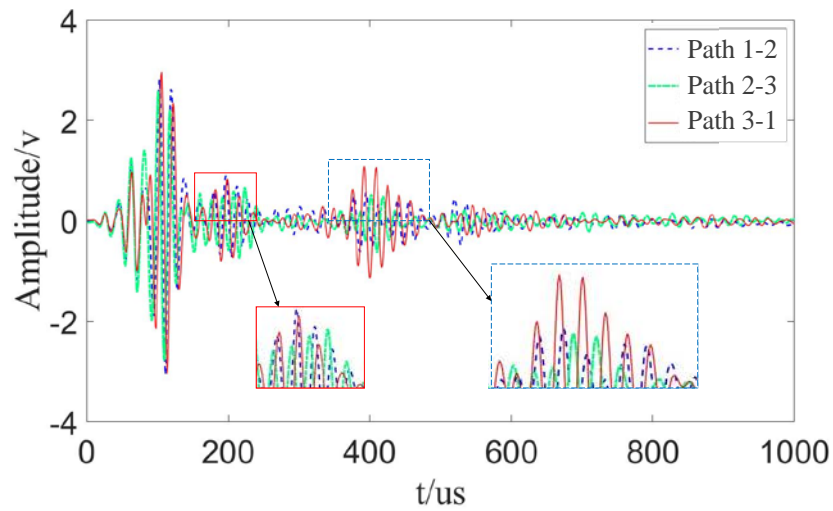


Figure 12. Wave signals captured by the three paths of the sparse sensor array when the damage is in region 1

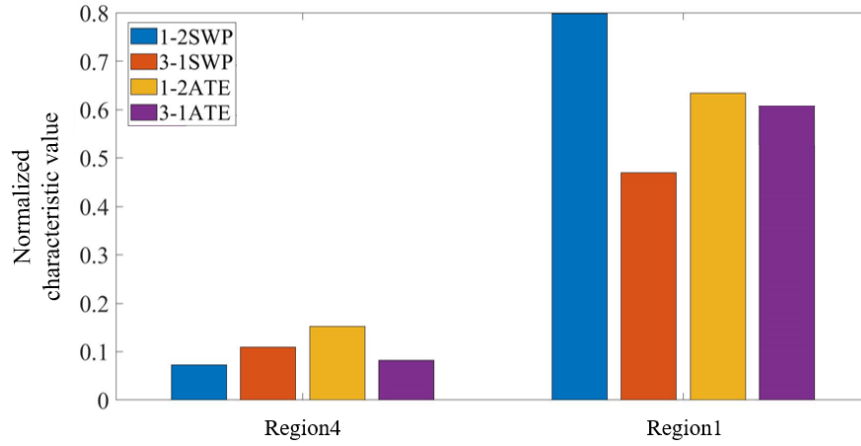


Figure 13. Histogram of characteristic parameters of region 4 and region 1

In the experiment, a total of 80 groups of wave signals are collected for each of the three regions (namely, regions 1, 2 and 4), and each group contains wave signals captured by the three sensing paths of the triangle-shaped sensor array. There are in total 240 groups of signals. Five multi signal features for each sensing path, including the time difference of arrival, the signal mutation time, the signal difference, the scattering signal size and the scattering wave packet, which are mentioned in Section 3.2 are extracted for further identification and localization of the damage.

The extracted wave features are employed as the input parameters to train and test the classification models using four different algorithms, including Decision Tree, Linear Discriminant, SVM and k-Nearest Neighbor (KNN). The training set and test set include 180 samples and 60 samples, respectively. In order to test the generalization ability of the model, the trained model is used to predict 60 groups of test dataset. The accuracy of prediction is shown in Table 2.

Table 2. Prediction accuracy of delamination damage positions

| Classification algorithm                   | T  | Corr | A     |
|--|----|------|-------|
| <b>Tree</b>                                |    |      |       |
| (Criterion: mse, Splitter: best)           | 60 | 50   | 83.4% |
| <b>Linear Discriminant</b>                 |    |      |       |
| (Solver: Lsq, Shrinkage: auto, Tol: 0.001) | 60 | 51   | 85%   |



|  |    |    |       |
|--|----|----|-------|
| <b>SVM</b>                               |    |    |       |
| <b>(Kernel: rbf, C: 1.0, Tol: 0.001)</b> | 60 | 53 | 88.3% |
| <b>KNN</b>                               |    |    |       |
| <b>(K: 5, Matric: minkowski)</b>         | 60 | 49 | 81.7% |

It can be found that the SVM outperforms the other three classification algorithms in the aspect of prediction accuracy, demonstrating that the SVM can be implemented for precise damage localization of composite structures.

#### 4.2 Damage degree prediction

Under external factors (i.e., mechanical and thermal loading, temperature and humidity change, service time of the structures), the structural damage will grow progressively, from embryonic stage, through mild and moderate stage to severe stage. The extracted features of the damage-scattered wave signals captured by the proposed triangle-shaped sensor array can be used to identify the severity and locate the position of the damage. In the experiment, 80 groups of wave signals are acquired for the four stages of the damage, resulting in a total of 320 groups of signals during the entire lifespan of the structure. 42 features of wave signals as listed in Table 1 are extracted from each sensing path, thus, a group of sensing waves captured by the sensor array contains 126 features. It is noteworthy that for the sake of data comparison, the magnitudes of the extracted wave features are normalized for each group of wave signals. Representative normalized wave features for a group of wave signals are displayed in Fig. 14.

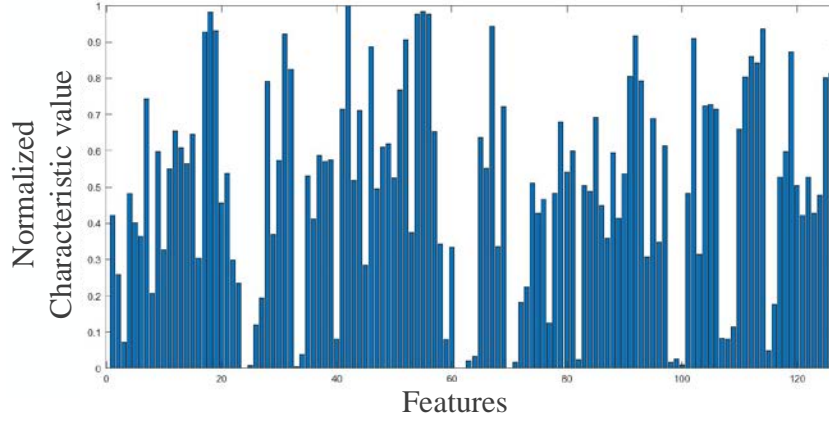


Figure 14. Normalization of wave characteristics parameters

Due to the high dimension of the extract wave features (320 groups of signals  $\times$  126 features of each group), the computation amount of the subsequent training of the damage degree prediction model will be extremely high if the original wave feature vectors are directly utilized as the input of classification algorithms. For this issue, the principal component analysis (PCA) is adopted to reduce the dimension of the wave feature vectors. By utilizing PCA, the original wave feature vectors are compressed and substituted for several unrelated principal components with retaining the majority of the information carried by these feature vectors.

Figure 15 shows the individual and cumulative contributions of the first 10 principal components of a wave feature vector after PCA processing, respectively. It can be observed that the cumulative contribution of the first 10 components is near 80%, indicating that the majority of the information of the wave feature vector can be revealed by the 10 components. Thus, the wave feature matrix is compressed from  $320 \times 126$  to  $320 \times 10$ , which will greatly improve the efficiency of the model training.

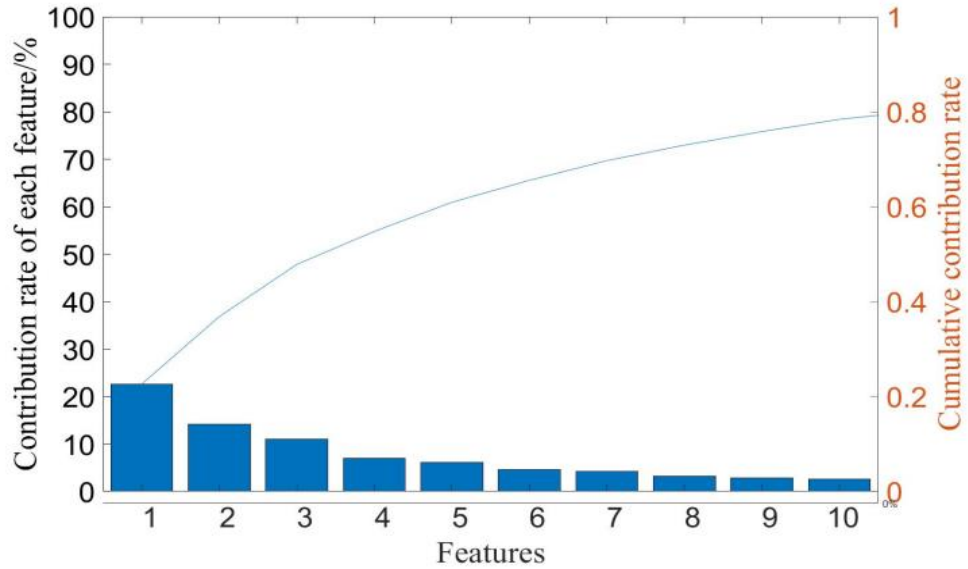


Figure 15. The individual and cumulative contributions of the first 10 principal components

The compressed wave feature vectors are employed as the input of the four classification algorithms compared in section 4.2.1, to train a prediction model for damage degree determination. Amongst the whole 320 wave feature vectors, 240 vectors are first used to train the prediction model, then the other 80 samples are employed to test the model. Table 3 illustrates the test results of the four algorithms.

Table 3. Prediction accuracy of delamination damage tracking evaluation

| Classification algorithm                   | Test | Correct predicti | Accuracy |
|--|------|------------------|----------|
| <b>Tree</b>                                |      |                  |          |
| (Criterion: mse, Splitter: best)           | 80   | 59               | 74%      |
| <b>Linear Discriminant</b>                 |      |                  |          |
| (Solver: Lsq, Shrinkage: auto, Tol: 0.001) | 80   | 68               | 85%      |
| <b>SVM</b>                                 |      |                  |          |
| (Kernel: rbf, C: 1.0, Tol: 0.001)          | 80   | 72               | 90%      |
| <b>KNN</b>                                 |      |                  |          |
| (K: 5, Matric: minkowski)                  | 80   | 60               | 75%      |

It can be observed that the prediction accuracy of SVM for the degree of delamination damage in composite structure is 90%, outperforming the other three algorithms. The test results demonstrate that by using the PCA-compressed wave feature vectors as the input of the SVM, the degree of structural damage in composites can be predicted with high accuracy.

## **5 Conclusions**

Considering the large number of sensors in conventional sensor array for large-scale structures and the resultant high extra weight and cost of equipment, a sparse, triangle-shaped sensor array is proposed in this study to identify, orientate and evaluate the degree of structural damage in composite structures. Lamb wave signal with damage information is obtained through the triangle sensor array. After multi angle observation and comparison in time domain, frequency domain, time domain and frequency domain, the more significant parameters that can reflect the damage characteristics are extracted and used as the input of the classification algorithm. Secondly, considering data redundancy, in order to improve computing efficiency, the PCA technology is adopted for parameter dimensionality reduction processing. The damage information can be retained greatly while the computing power is reduced. The processed parameters are used to train the machine learning model. Finally, the accuracy of the scheme is verified by predicting the random unknown damage. Proof-of-concept experiment is performed to acquire the Lamb wave signal database for the training and test of the model. The test results show that the trained model can orientate and characterize the degree of the damage with high accuracy, demonstrating that by using the multiple features of Lamb wave signals, the reduction of damage information caused by the lower sensors in the triangle-shaped sensor array can be well compensated. By comparing the prediction accuracy of different classification algorithms, it is found that the SVM outperforms other algorithms, indicating that the combination of the triangle-shaped sensor array and SVM can effectively facilitate the damage identification and characterization of large-scale structures

with small amount of sensors.

However, there still exist some limitations for the proposed method. Comparing with traditional damage localization methods, such as Delay And Sum (DAS) imaging, this method could only give an estimated region of damage. And, further research is still worthy to address the layout optimization of triangle-shaped sensor arrays to improve the damage estimation accuracy, when damage is occurred near the structure boundary or inside the triangle-shaped sensor array. Also, the optimum parameters of SVM will be studied through a large amount of data analysis in the future research.

## References

1. Surace Cecilia. Special Issue on Novel Approaches for Structural Health Monitoring. *Applied Sciences*2021; 11(16):7210-7210.
2. Ghosh T, Kundu T. A new transducer holder mechanism for efficient generation and reception of Lamb modes in large plates. *Journal of the Acoustical Society of America*1998; 104(3):1498-1502.
3. Jagannathan R. Krishnan B. Krishnamurthy C V. A single transmitter multi-receiver (STMR) PZT array for guided ultrasonic wave based structural health monitoring of large isotropic plate structures. *Smart Materials and Structures*2006; 15(5):1190-1196.
4. Kundu T. Nakatani H. Takeda N. Acoustic source localization in anisotropic plates. *Ultrasonics*2012; 52(6):740-746.
5. Yin S. Cui Z. Kundu T. Acoustic source localization in anisotropic plates with ‘Z’ shaped sensor clusters. *Ultrasonics -London Then Amsterdam*2018; 84(1):34-37.
6. Campeiro L M. Budoya D E. Baptista F G. Lamb wave inspection using piezoelectric diaphragms: An initial feasibility study. *Sensors and Actuators*2018; 331:131-132.
7. Salamone S. Bartoli I. Di Leo P. Lanza Di Scalea F. Ajovalasit A. D'Acquisto L. Rhymer J. Kim H. High-velocity impact location on aircraft panels using macro-fiber composite piezoelectric rosettes. *Journal of Intelligent Material Systems and Structures*2010. 21: 887-896.
8. Howard M Matt. Francesco Lanza di Scalea. Macro-fiber composite piezoelectric rosettes for acoustic source location in complex structures. *Smart Materials and Structures*2007. 16(4):1489-1499.

9. Yin S, Xiao H, Cui Z, Tribikram Kundu. Rapid localization of acoustic source using sensor clusters in 3D homogeneous and heterogeneous structures. *Structural Health Monitoring* 2021;20(3):1145-1155.
10. Xue C. Xu G, Wang X. Gao J. Gao D. Error analysis and correction of multi-sensor cluster methods for acoustic emission source localization. *Ultrasonics*2021; 115(1):106438-106446.
11. Su L. He H. Seismic vulnerability assessment for RC frame structure based on SVM. *Journal of Huazhong University of Science and Technology*2018; 46(5)115-120.
12. Noori H A. Rashidi M. Liyanapathirana R. Samali B. Algorithm Development for the Non-Destructive Testing of Structural Damage. *Applied Sciences*2019; 9(14):2810-2815.
13. Thirumalaiselvi A. Sasmal S. Pattern recognition enabled acoustic emission signatures for crack characterization during damage progression in large concrete structures. *Applied Acoustics*2021; 175(1):107797-107812.
14. Bolourani A. Bitaraf M. Nekouvaght T A. Structural health monitoring of harbor caissons using support vector machine and principal component analysis. *Structures*2021; 33(1):4501-4513.
15. Yang Z. Radzienski M. Kudela P. Ostachowicz W. Fourier spectral-based modal curvature analysis and its application to damage detection in beams. *Mechanical systems and signal processing*2017; 84(1):763-781.
16. Yang Z. Radzienski M. Kudela P. Ostachowicz W. Two-dimensional modal curvature estimation via fourier spectral method for damage detection. *Composite Structures*2016; 148:155-167.
17. Zhang Y. Zhang X. Chen J. Development on detecting technique of structure damage based on EMI. *Nondestructive Testing*2016; 16(1):69-74.
18. Patricia da Silva Lopes Alexandrino et al. A robust optimization for damage detection using multiobjective genetic algorithm, neural network and fuzzy decision making. *Inverse Problems in Science and Engineering*202; 28(1):21-46.
19. Hossain M S. Ong Z C. Ismail Z. Noroozi S. Khoo S Y. Artificial neural networks for vibration based inverse parametric identifications: A review. *Applied Soft Computing*2017; 52(1):203-219.
20. Mario A. de Oliveira. Daniel J. Inman. Performance analysis of simplified fuzzy artmap and probabilistic neural networks for identifying structural damage growth. *Applied Soft Computing*2017; 52(1)53-63.

21. Wang P. Shi Q. Tao C. Damage identification in structures based on energy curvature difference of wavelet packet transform. *Shock & Vibration*2018; 2018: 1-13.
22. Zhang W. Sun L. Zhang L. Local damage identification method using finite element model updating based on a new wavelet damage function. *Advances in Structural Engineering*2018; 21(10):1482-1494.
23. Barchi F. Zanatta L. Parisi E. Burrello A. Brunelli D. Bartolini A. Acquaviva A. Spiking Neural Network-Based Near-Sensor Computing for Damage Detection in Structural Health Monitoring. *Future Internet*2021; 13(8):219-219.
24. Mousavi M. Gandomi A H. Structural health monitoring under environmental and operational variations using MCD prediction error. *Journal of Sound and Vibration*2021; 521:116370-116382.
25. Kanji O. Structural Health Monitoring of Large Structures Using Acoustic Emission – Case Histories. *Applied Sciences*2019; 9(21):455-459.
26. Si L. Li Z. Online structural state assessment for aerospace composite structures using an acousto-ultrasonics-based multi-damage index identification approach. *Structural Health Monitoring*2020; 19(6):1790-1807.
27. Lee Y. Park J. Lee D. Inspection interval optimization of aircraft landing gear component based on risk assessment using equivalent initial flaw size distribution method. *Structural Health Monitoring*2020; 18(6): 124-142.
28. Li H. Spencer B F. Rao AS. Nguyen T. Palaniswami M. Ngo T. Vision-based automated crack detection using convolutional neural networks for condition assessment of infrastructure. *Structural Health Monitoring*2020; 20(4):2124-2142.
29. Pan Y. Hong R. Chen J. et al. Performance degradation assessment of wind turbine gearbox based on maximum mean discrepancy and multi-sensor transfer learning. *Structural Health Monitoring*2020; 20(2):118-138.
30. Fallahian M. Khoshnoudian F. Meruane V. Ensemble classification method for structural damage assessment under varying temperature. *Structural Health Monitoring*2017; 17(4): 747-762.